DOI: 10.26599/FSHW.2025.9250568

Contents lists available at SciOpen

Food Science and Human Wellness

journal homepage: https://www.sciopen.com/journal/2097-0765

China Food Publishing Co.

Pterostilbene modulates diurnal acetylation in mouse liver to ameliorate sleep restriction induced metabolic disorders *via* restoring circadian-dependent SIRTs activity

Yuqing Liu, Jun Zhang, Qian Bai, Xiaolei Wang, Chang Luo, Long Yi, Mantian Mi，Ka Chen*

Research Center for Nutrition and Food Safety, Chongqing Key Laboratory of Nutrition and Health, Institute of Military Preventive Medicine, Third Military Medical University (Army Medical University), Chongqing 400038, China.

ABSTRACT: Sleep restriction (SR) poses a significant risk for metabolic disorder, correlating to perturb circadian clock. Lysine protein post-translational modifications (PTMs), reversibly modified by the acyltransferases and deacetylases, are identified to regulate metabolic processes in a circadian-dependent manner. Pterostilbene (PTE), a stilbene analogue to resveratrol, had been primarily proved to mitigate metabolic disorders. Thus, it is meaningful to understand how lysine PTMs affected metabolism under SR condition and elucidate the underlying mechanisms of PTE in PTMs perspective. Herein, we firstly revealed that PTE improved systemic energy homeostasis, liver metabolic and mitochondria function of mice subjected to 5-days' SR in a diurnal range. Then, we primarily screened out that acetylation was the remarkable alteration among the 11 types of lysine PTMs in the livers from SR mice at ZT4 and ZT16. With further LC-MS/MS-based acetylome analysis, 4880 acetylation sites on 1370 proteins were identified, and nearly 50% differentially expressed Kac-modified proteins (DEAPs) were located in the mitochondria. Subsequent analysis demonstrated that PTE could mitigate SR-induced diurnal acetylation disruption of functional proteins related to metabolism, with notably relieving SR-induced inhibition in "amino acid metabolism" and "lipid metabolism" at ZT4. Moreover, PTE could normalize the diurnal expression and activity of deacetylases SIRT1/3 by maintaining NAD^+ oscillation thus modulating acetylation. Our work represents a comprehensive resource detailing the acetylation modification responded by the liver in sleep deficiency, and provides substantial evidence to illustrate the mechanisms of PTE on SR-induced metabolic disorders.

Keywords: Pterostilbene; sleep restriction; metabolic disorder; mitochondrial dysfunction; lysine acylation modification; Sirtuins

1. Introduction

Various stresses in modern society cause nearly half of adults not getting enough sleep, and SR has been proved to be an independent risk factor for metabolic syndrome as initially triggering metabolic disorders including the rise of blood glucose/lipids and insulin resistance [1-3]. Therefore, the quest for efficacious strategies to mitigate metabolic disorders induced by SR persists. Recently, the metabolic improvement effects of phytochemicals such as resveratrol and nobiletin have attracted attention[4-6]. PTE (trans-3, 5-dimethoxy-4-hydroxystilbene), abundantly existing in a traditional Chinese medicine *dragon's blood* and

***Corresponding author**
chenka@tmmu.edu.cn

Received 3 December 2024
Received in revised from 25 December 2024
Accepted 2 February 2025

several fruits (e.g. grape, blueberry and strawberry), is a stilbene structurally similar to resveratrol. Besides its powerful antioxidant and anti-inflammatory properties[7], PTE has been found to have anti-obesity effects *via* increasing basal metabolic rate and/or altering lipid metabolism in a mitochondrion-dependent manner[8-10]. Moreover, our previous studies have primarily found that PTE could protect against SR-induced metabolic disorders and exercise intolerance [11-12]. However, the underlying mechanism of its metabolic improvement effects under SR condition remains unclear.

A molecular clock network is vital for maintaining metabolism homeostasis. Currently, lysine protein post-translational modifications, such as acetylation (Kac), butyrylation (Kbu) and malonylation (Kma), are identified to dynamically regulate metabolic processes in a circadian-dependent manner[13-14]. For example, acetylation of clock proteins (BMAL1-K537) directly modulates liver circadian rhythms *via* converting metabolites signals into changes in protein regulatory function, and proteomewide surveys display a number of mitochondrial proteins involved in versatile metabolic pathways including glycolysis/gluconeogenesis, citric acid cycle, amino acid metabolism and fatty acid metabolism are heavily influenced by clock-driven acetylation[15-18]. Acute sleep-wake cycle disruptions caused by SR can perturb circadian clock, however, less are known about how SR affects lysine PTMs and its interplay with metabolism. PTMs regulation revolves around modification reversibility, implying that two types of enzymes as the “writers” and “erasers” specifically add or remove the modification to targeted (modified) amino acid residues. The intracellular acylation levels are maintained by the “writers” lysine acyltransferases (KATs) and the “erasers” lysine deacetylases (HDACs). Nicotine adenine dinucleotide^{+} (NAD^{+})-dependent sirtuin deacetylases (SIRTs), the class III HDACs, are found to regulate critical signaling pathways in numerous metabolic processes[19]. Previous studies have revealed that PTE could ameliorate western diet-induced obesity or high-fat-diet-induced lipid accumulation exacerbated by chronic jet lag *via* SIRT1 and SIRT3 activation[20-21]. Moreover, some researchers hypothesized that SIRTs might be the directly target of PTE to influence Kac rhythm of liver proteins[9,22]. Thus, it is necessary to further elaborate the relationship between PTE and SIRTs in modulation the lysine PTMs under SR condition.

In the present study, we were firstly set to investigate how PTE intervention affected the systemic energy homeostasis and liver metabolic function in a diurnal range. Then, using a panel of pan antibodies, we primarily depicted the alterations of 11 types of the novel identified lysine acylation modifications (eg. Kac, Kbu, Kma, et al) in liver proteins of SR mice. As remarkable changes were observed in Kac modification with PTE intervention, the LC-MS/MS-based quantitative proteomics approach was further used to profile the diurnal rhythms of Kac and particularly analyzed the Kac modification in featured metabolism related proteins. Furthermore, we investigated the influence of PTE on the circadian expression and activity of lysine deacetylases SIRT1 and SIRT3 to demonstrate the underlying mechanism. Our work will firstly decipher the global characterization of lysine PTMs in liver of SR mice, and provide substantial evidence to illustrate the beneficial effects and mechanisms of PTE on SR-induced metabolic disorders.

2. Experimental details

2.1 Animals

C57BL/6J male mice (Hunan STJ Laboratory Animal Co., Ltd, China) at eight weeks age were housed under controlled ambient temperature of (22 ± 2)℃ and humidity of (55 ± 5)%, providing with standard chow diet and water ad libitum. Mice were routinely raised under 12h: 12h light-dark cycle, consisting of lights on at 8:00 defined as Zeitgeber time 0 (ZT0) and lights off at 20:00 defined as ZT12.

Subsequently, mice were randomly assigned into three groups: control group (CON), sleep-restriction group (SR) and sleep-restriction + pterostilbene group (SR+PTE), with 60 mice in each group. SR mouse models and PTE supplementation were implemented as previously described [11]. Briefly, after 7-day adaptation period, SR and SR+PTE mice were restricted sleep daily for 20 h (ZT 12 to the following ZT 8) in 5 consecutive days with a sleep-disrupted instrument (SANS Biological Technology, China). Animals in CON group were allowed to sleep under the same conditions optionally in the rectangle cages. The supplemented dose of PTE (HPLC ≥ 98%, Must biotechnology, China) in this study was 100mg/kg·bw administration[错误!未找到引用源。], dissolved in 0.9% normal saline and given once a day by gavage at ZT1.

At the end of the SR mouse model establishment, all mice were sacrificed with 2% chloral hydrate. Serum and liver tissues from three groups were excised at ZT0, ZT4, ZT8, ZT12, ZT16, ZT20 and ZT24, then stored at –80˚C for further analysis. Animal care and experiment protocols in this research were in accordance with the Animal Care and Use Committee of Third Military Medical University (AMUWEC2020728, March 31, 2020).

2.2 Body weight, Food intake and Body mass composition

The body weight was examined at ZT1 every day. Food intake was calculated through dividing the feed consumption each day by the number of mice in each group of mice fed with mouse maintenance feed (Xietong, China). Fat, lean and water body mass were measured by a nuclear magnetic resonance (NMR) spectrometer (Niumag Analytical Instrument Corporation, China). The data were calculated automatically by the instrument software (Niumag NMR Animal Body Composition Analysis software V3.0) and expressed in grams and percentages.

2.3 Metabolic cage data acquisition

Indirect calorimetric analysis was performed as operating instructions by TSE System for Small Laboratory Animals (PhenoMaster, Germany). In short, mice were given standard chow and water ad libitum, and separated cages under 12h: 12h light-dark cycle after mice models establishment, immediately. The CaloSys module was used to assess indirect calorimetry and energy balance parameters, including CO_2 production, O_2 consumption, respiratory exchange rate (RER) and heat production. All date were measured every 2 minutes for up to 5 consecutive days at a room temperature.

2.4 Serum biochemical indexes

The serum biochemical indexes including alanine aminotranferse (ALT), aspartate aminotranferse (AST), total bile acid (TBA), lactate pehydrogenase (LDH), creatine kinase (CK) and creatine kinase-MB

(CK-MB) were detected by HITACHI 3100 automatic analyzer (HITACHI, Japan). All test assay kits matched with the instrument were from purebio labaties (PREB, China).

2.5 Liver lipid content and ATP concentration

Liver total cholesterol (TC), triglyceride (TG), free fatty acid (FFA) and ATP concentration were followed the commercial ELISA kits (Solarbio, BC-1980, BC-0620, BC-0595, China and Beyotime, S0027, China).

2.6 Transmission electron microscopy (TEM) observation

Mitochondrial morphology in the liver was observed by TEM. Briefly, liver samples from ZT4 mice were cut as 1 cm^3, fixed in 1% osmium tetroxid, dehydrated and subsequently embedded. After staining with 2% uranyl acetate and lead citrate, ultrathin sections were observed under a JEM-1400 microscope (Jeol, Japan).

2.7 RNA extraction and Real-Time quantitative PCR (RT-qPCR)

Total RNA from frozen liver tissues was extracted according to the manufacturer's Trizol protocol (Ambion, USA). NanoDrop (Thermo Fisher, NANODROP2000, USA) was used to measured concentration, and synthesised complementary DNA (cDNA) was synthesized from 1 μg RNA by PrimeScript RT Master MIX (TaKaRa, Japan). RT-qPCR was performed using TB Green Premix Ex TaqII (TaKaRa, Japan) with Quant Studio 3 real-time PCR instrument (Thermo Fisher Scientific, USA). Relative quantities of mRNA expression were normalized to the geometric mean of 18sRNA values by the $2^{-\Delta\Delta Ct}$ method. The primer sequences are shown in Table S1.

2.8 Protein extraction and western blotting

Frozen liver specimens were homogenized in RIPA lysis buffer with the presence of 500 μmol/L PMSF (serine protease inhibitor) and 20 mmol/L NaF (phosphatase inhibitor). Total protein concentration in liver extracts was measured using the BCA Protein Assay Kit (Beyotime, China). Protein extracts were separated by 10% SDS-polyacrylamide gel electrophoresis (SDS-PAGE) gel and transferred onto a polyvinylidene difluoride (PVDF) membrane (Millipore, USA). Before incubating with primary antibodies summarized in Table S2 overnight at 4°C, all membranes were immersed in QuickBlock™ Blocking Buffer (Beyotime, China) for 20 min at room temperature. HRP-conjugated goat anti-mouse IgG antibody and goat anti-rabbit IgG antibody were chosen to detect with proteins of interest. Peroxidase substrate was provided by High ECL Enhanced Western Blotting Substrate (Bio-Rad, China), blots were visualized by ChemiDoc Touch Imaging System (Bio-Rad). Densitometric analyses were performed by the ImageJ software v5.21.

2.9 Global lysine acetylation modification analyses

An integrated method involving bio-material-based PTM enrichment (for acetylation) and LC-MS/MS were used to quantify the dynamic changes in the whole acetylome. Experimental technical and bioinformatics analysis was supported by the PTM Biolab (Hangzhou, China). See concrete details in the Supplemental methods.

2.10 SIRT1 activity assay and NAD⁺ concentration

According to the manufacturer's instruction, SIRT1 activity and NAD^+ concentration was assessed with the CycLex SIRT1 Deacetylase Fluorometric Assay Kit Ver.2 (MBL, CY-1151V2, Japan) and NAD^+/NADH Quantification Kit (SIGMA, MAK037, USA).

2.11 Statistical analysis

Ordinary one-way ANOVA followed by Bonferroni's multiple comparisons test was used to compare the statistical significance of differences between any two groups with one variable. Two-way ANOVA followed by Tukey's multiple comparisons test was used to determine the statistical significance among experimental groups with different ZT, including metabolic cage data, SIRT1 enzyme activity, NAD^+ content and gene transcription and protein expression level. Cosine analysis was depended on the website (https://wong-zjyi.shinyapps.io/Consinor_Analysis_of_Rthyms/) and the software Cosinor (version 3.1). The function was defined as $f(x) = M + A \cos(2\pi T/x - ø)$, including variables M (Mesor; mean statistics of rhythm), A (Amplitude, half of the total peak-trough variation), T (Period, 24 h under LD 12/12) and ø (Acrophase, elapsed time from ZT0), and the differences between any parameters following F-test method. Fisher's exact test was used to analyze the function enrichment significance of differentially expressed proteins (with the identified proteins as the background). All figures and statistical analyses were performed by GraphPad Prism (Ver. 8.0.2; GraphPad Software, San Diego, CA, USA). All data are expressed as mean ± SD. All experiments were repeated at least three times and $P < 0.05$ was considered significant.

3. Results

3.1 PTE maintained systemic energy metabolism balance under SR

Previous study reported that PTE increased energy expenditure and maintained the balance of nutrient metabolism in obese-related mouse models[10]. In our previous study, we have found that middle (100mg/kg) and high (200mg/kg) dose PTE could improve metabolic disorders induced by SR, similar as the effects of the hypolipidemic and hypoglycemic drugs (atorvastatin and rosiglitazone)[12] , and the dose of 100mg/kg was used in the present study. In this study, we were set to further investigate how PTE affected the circadian-dependent energy metabolism and specifically on the lysine PTMs (Figure 1).

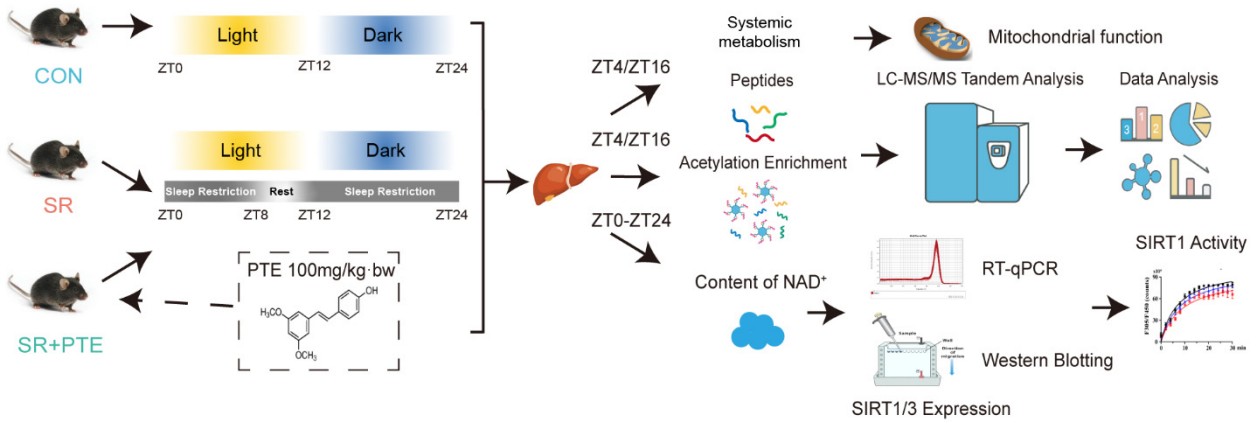

Figure 1. Schematic diagram showing the study process for the protective effects of PTE on metabolic disorders and acetylation modification of liver proteins under SR.

As shown in Figure 2A-2C, PTE intervention was confirmed to sufficiently inhibit the body weight and food intake reduction caused by 5-day sleep restriction. Moreover, according to the body mass composition assay, we found that PTE intervention could reduce SR-induced elevation of the fat mass on condition of the body weight loss (Figure 2D-2G), suggesting its special role in lipid metabolism under SR. Further, indirect calorimetric analysis was implemented to evaluate the systemic metabolic status of SR mice in consecutive 5 days after SR treatment (Figure 2H-2K). Remarkably higher VCO_2, RER and heat production were observed in the rest phase (ZT0-ZT12) in the SR group, suggesting that substrate preference for more carbohydrate. Compared with the SR group, PTE intervention significantly reduced VCO_2, RER and heat production in the rest phase, indicating its effectiveness on enhancing lipid consumption and maintaining the metabolic substrate selection balance. Collectively, these results demonstrated that PTE could maintain systemic energy metabolic homeostasis under SR *via* particularly improving lipid metabolism.

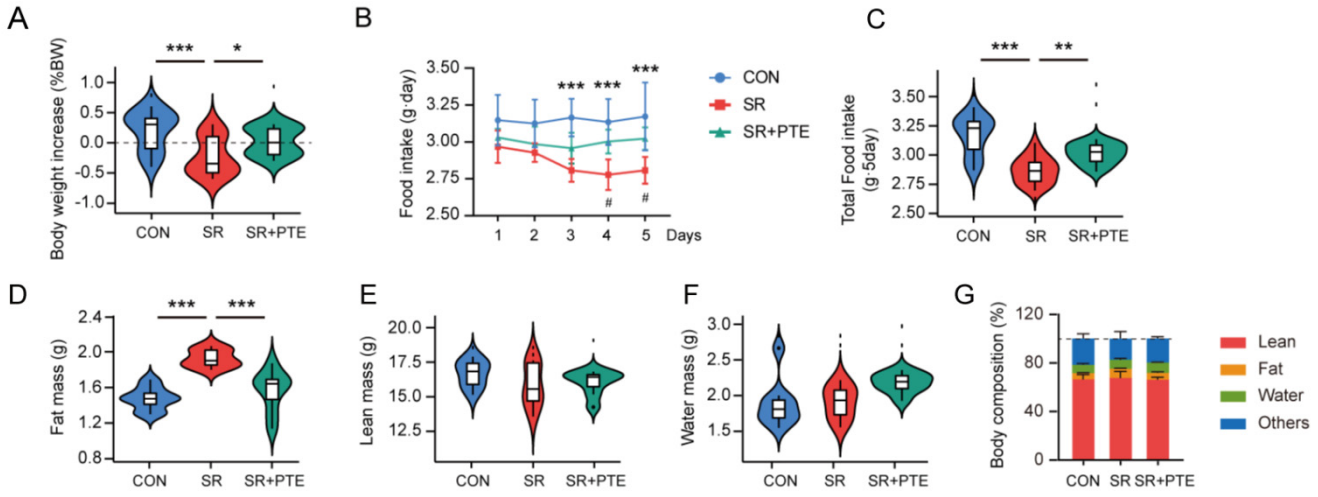

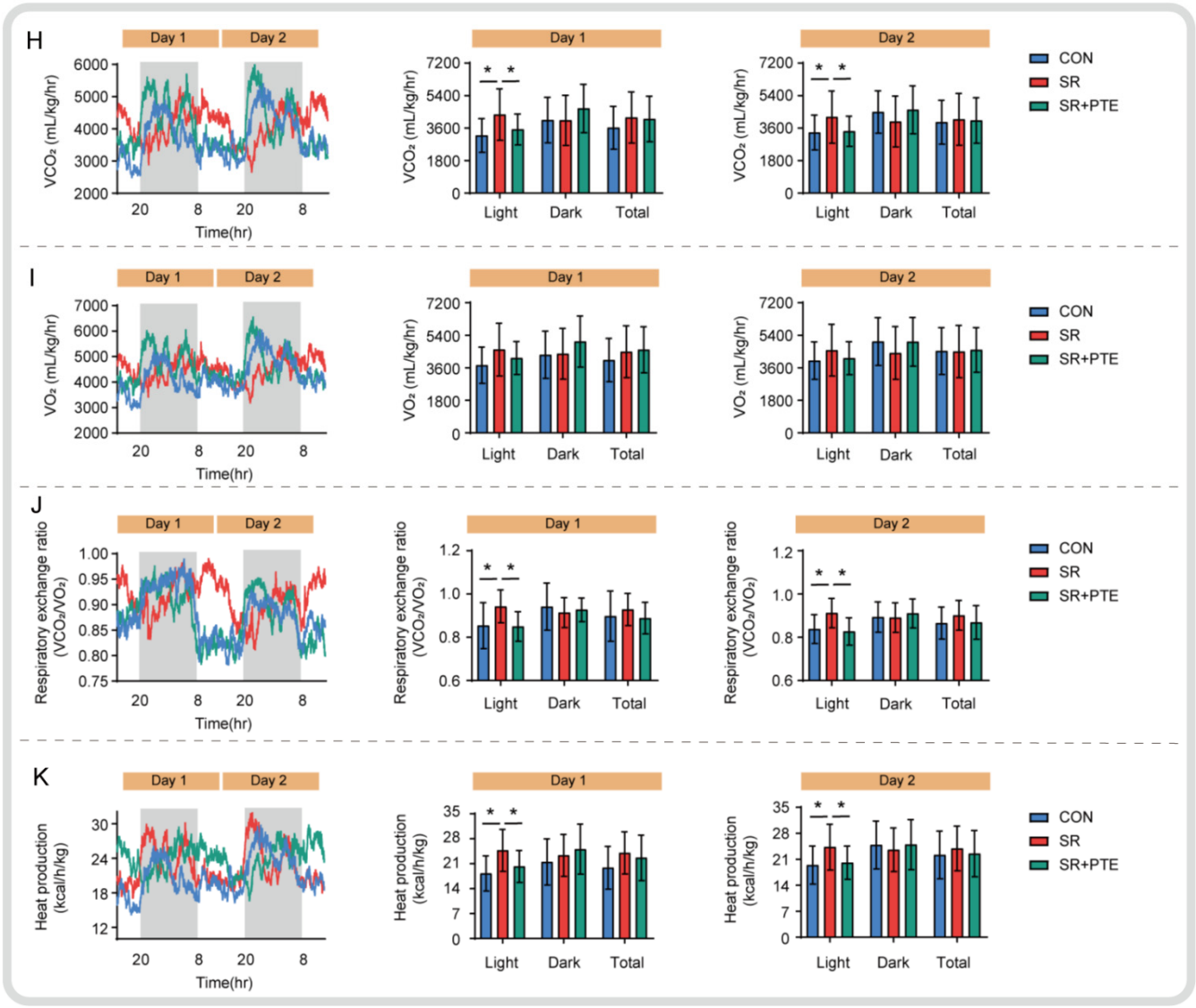

Figure 2. PTE maintained energy metabolism balance under SR.

(A) Changes in body weight before and after SR (n = 16). (B,C) Food intake of SR mice and treated with PTE for 5 days (n = 16). (D-G) Body mass composition (fat, lean, water) for the above three groups of mice analyzed by NMR spectrometer (n = 8). Indirect calorimetric analysis data including the diurnal rhythms of VCO_2 (volume of carbon dioxide production) (H), VO_2 (volume of oxygen consumed) (I), RER (J) and heat production (K) and their analysis during light, dark and total phase for the above three groups of mice (n = 8). Data are presented as mean ± SD, and statistics were performed with one-way ANOVA, $*P < 0.05$,$**P < 0.01$, $***P < 0.001$.

3.2 PTE improved hepatic metabolism in SR mice

As for the liver is the key metabolic organ, we next sought to investigate the influence of PTE on liver metabolism. Firstly, we confirmed that PTE treatment substantially improved SR-induced hyperglycemic state as evidenced by the reduction of the fasting blood glucose and increased liver glycogen at ZT4 (Figure 3A-3D). Then, we found that PTE intervention decreased liver TC content at ZT4 and ZT16, as well as liver FFA content at ZT4 (Figure 3E-3G). Further, RT-qPCR analysis and immunoblot analysis were used to investigate the effects of PTE on the lipid metabolic biological process. As shown in Figure 3H, PTE heightened the transcription levels of the key transcriptional factors (*Ppara*, *Pparg*) in lipid metabolism at ZT4, and reduced the hepatic glycolysis genes expression, including *Atgl* at ZT4, as well as *Pfk*, *Gck* at ZT4

and ZT16 in the liver of SR mice. As shown in Figure 3I-3J, PTE decreased the protein expression of lipid metabolic enzymes and transcription factors, such as ACC1, HMGCR2 at ZT4 and increased PPARγ expression at ZT4 and ZT16, which could contribute to the lower liver lipid levels under SR condition. Nevertheless, PTE intervention did not show significant difference in lipid transporters FFAR2 nor FFAR3 protein expression. Additionally, as extra fatty acid or cholesterol accumulated in hepatocytes would lead to liver damage[23], some indexes reflecting the liver function were determined. The abnormally elevated serum TBA, CK and LDH activity, reflecting the substantial liver damge, were reversed by PTE (Figure S1A-S1F). Meanwhile, SOD activity was dramatically increased with PTE intervention under SR, and MDA level was reduced by PTE at ZT4 (Figure 4A-4B). Thus, the liver function improvement might be partially attributed to lipid metabolic homeostasis kept by PTE. Together, the results above demonstrated that PTE mitigated liver glucose/lipid metabolism and had some hepatoprotective effects under SR condition.

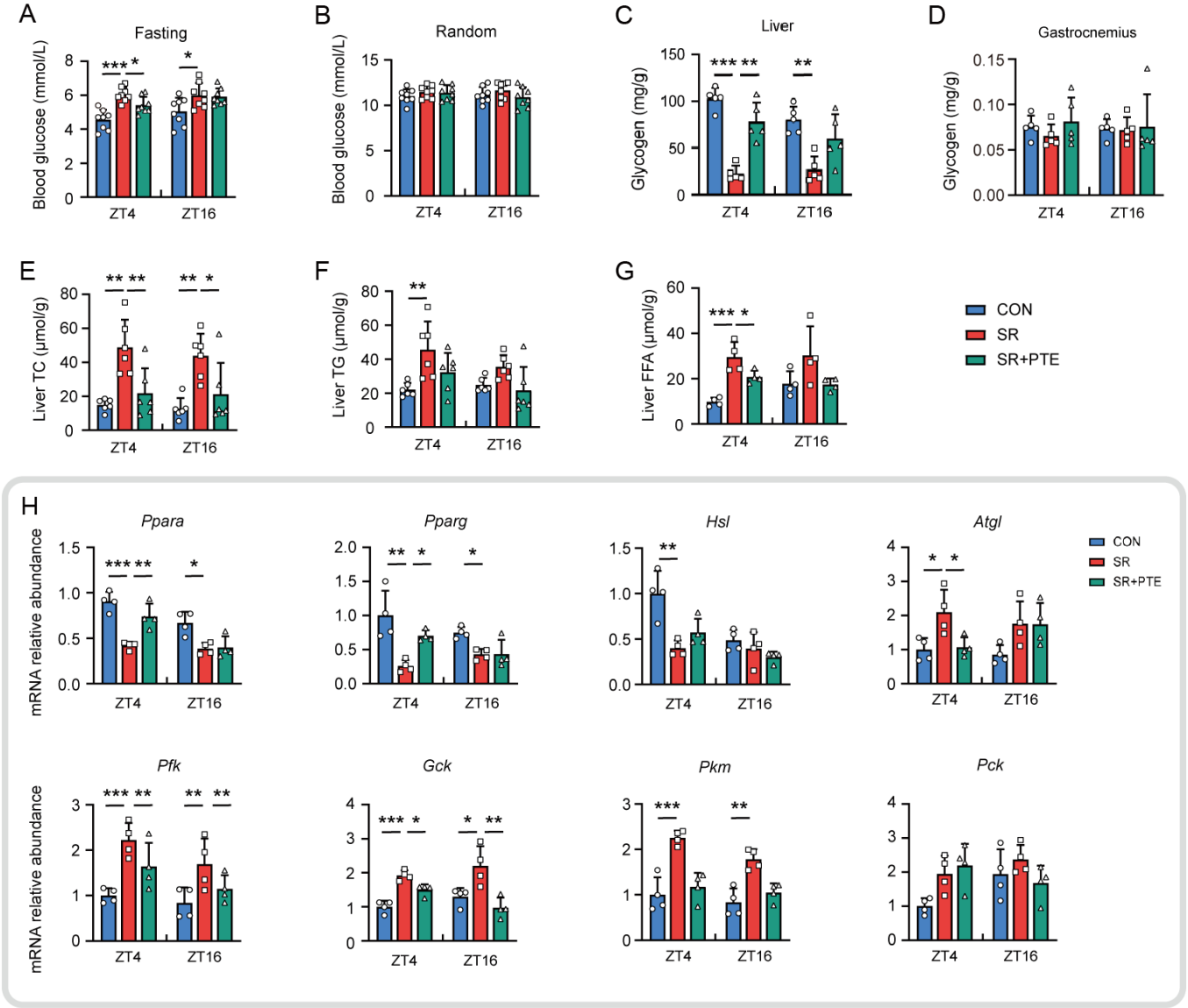

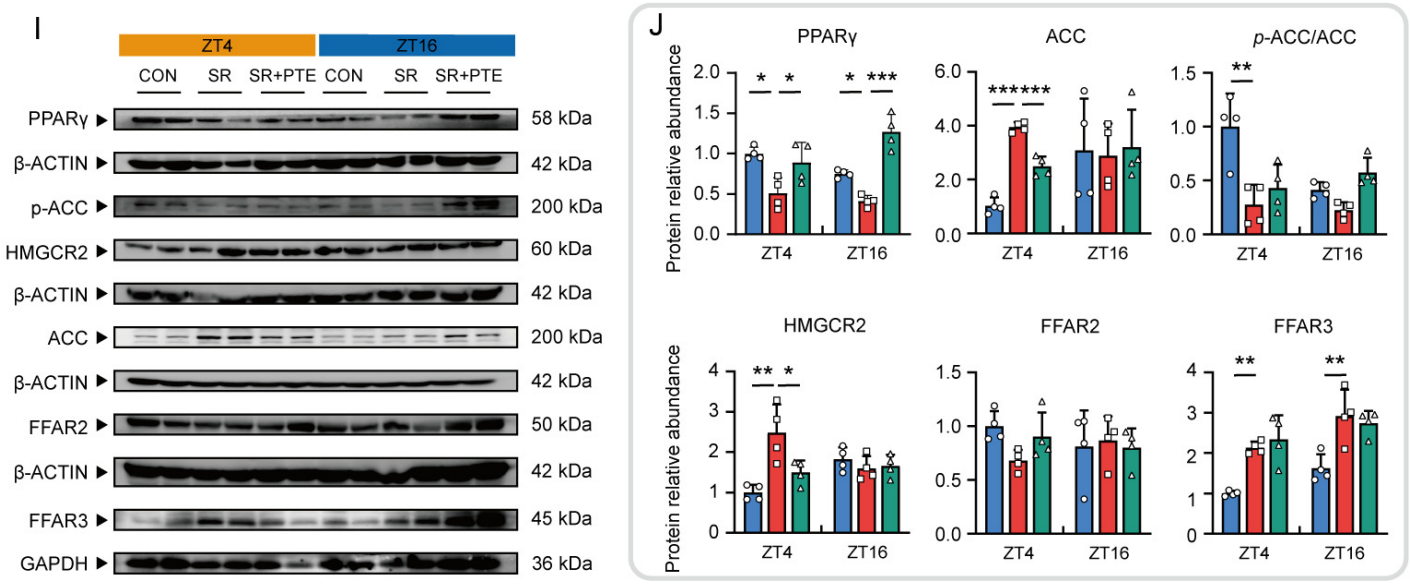

Figure 3. PTE mitigated ectopic fat deposition in the liver of SR mice.

(A,B) Fasting and random blood glucose levels in PTE- intervened SR mice at two opposite time points (n=8). (C,D) Liver and gastrocnemius glycogen at ZT4 and ZT16 (n=5). (E-G) Total TC, TG, FFA levels in the livers (n=4-6). (H) Real-time qPCR analysis of mRNA expression of glycolysis and lipid metabolism genes in the livers (n=4). (I,J) Western blotting analysis were performed to measure protein expression of lipid metabolism (n=4). Data are presented as mean ± SD, and statistics were performed with one-way ANOVA, $*P < 0.05$,$**P < 0.01$, $***P < 0.001$.

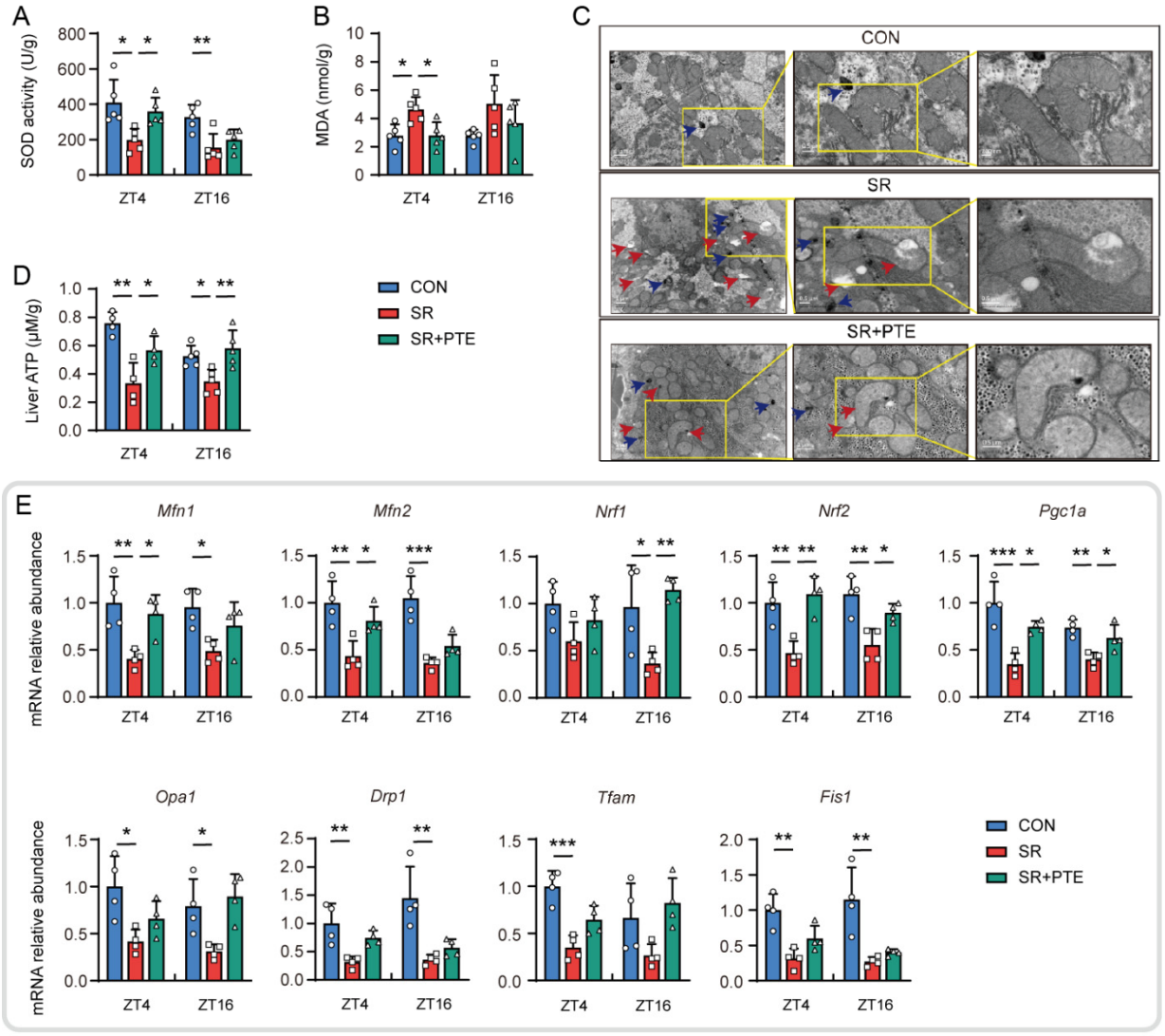

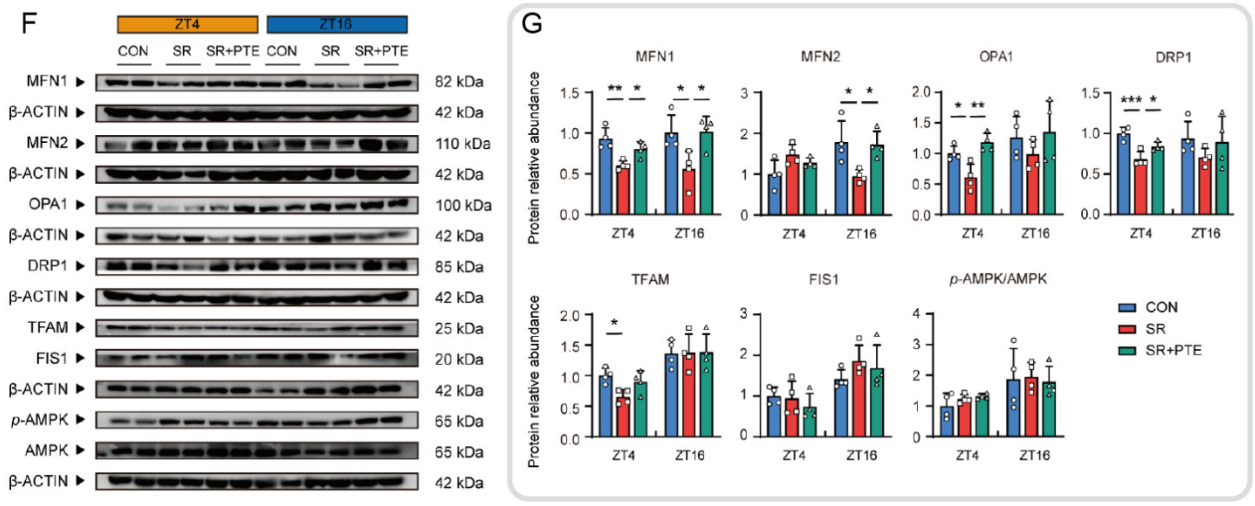

Figure 4. PTE improved mitochondrial dysfunction in the liver of SR mice.

(A,B) SOD activity and MDA content in the livers were determined by ELISA kits at two opposite time points (n=5). (C) Representative TEM images of mitochondria in whole livers from SR mice after 5 days treatment. The red arrows indicated swollen mitochondria, and black arrows indicated lipofuscin (n=4). (D) ATP content in the livers from three groups mice (n=4-5). (E-G) Real-time qPCR and western blotting analysis of transcription and protein expression of mitochondrial dynamics related genes in the livers (n=4). Data are expressed as the mean ± SD. Statistics were performed with one-way ANOVA, *$P < 0.05$, **$P < 0.01$, ***$P < 0.001$.

3.3 PTE mitigated mitochondrial dysfunction in the liver of SR mice

Given the essential role of mitochondrion in energy metabolism, we next to explore the effects of PTE on SR-induced mitochondrial dysfunction. According to the ultrastructure of mitochondrion (Figure 4C), we found that PTE improved mitochondrial damage and reduced lipofuscin formation in SR livers at ZT4. The quantitative analysis of mitochondrial ATP revealed that PTE significantly suppressed liver ATP reduction at ZT4 and ZT16 (Figure 4D). RT-qPCR analysis further illustrated PTE affected the mitochondrial fusion and fission related genes expression. For example, the decrease of fission genes (*Mfn1* and *Mfn2*) transcription expression was prevented by PTE at ZT4, biosynthetic genes *Nrf1* at ZT16, as well as biosynthetic genes *(Nrf2* and *Pgc1a*) at both ZT4 and ZT16 (Figure 4E). Consistently, PTE also altered the protein expression involved in mitochondrial fusion and fission (MFN1, MFN2, DRP1 and OPA1), whereas PTE did not significantly change the level of p-AMPK (Figure 4F-4G). Together, these findings demonstrated that PTE has a mitochondrial-protective effect to mitigate SR-induced mitochondrial dysfunction.

3.4 PTE altered the comprehensive landscape of Kac in the liver of SR mice at ZT4

PTMs play a critical role in modulating biological processes in response to acute environmental signals. To investigate the involvement of PTMs in SR-induced liver pathophysiology, a serial of lysine acylation modifications was primarily determined in SR mouse liver using a panel of pan antibodies. As shown in Figure S2, the 11 types of newly identified PTMs, including Kac, Kbu, Kma, lysine succinylation (Ksucc), lysine β-hydroxybutyrylation (Kbhb), lysine crotonylation (Kcr), lysine 2-hydroxyisobutyrylation (Khib), lysine benzoyl (Kben), lysine propionylation (Kpropi), lysine lactation (Klac) and lysine glutarylation (Kglu) had shown some alterations. Among them, Kac, Kcr and Kbhb were seemed to have circadian alteration and affected by PTE, and Kac was the one remarkablely changed in response to SR. To better understand the

global landscape of Kac in mouse livers, liver tissues at ZT4 and ZT16 were subjected respectively to systematic quantitative Kac proteomic analyses. Sample quality control (QC) showed excellent reproducibility of the proteomic datasets, including relative standard deviation (RSD), the Pearson correlation coefficient (PCC), Principal component analysis (PCA), as well as the peptide length distribution, protein coverage and number of peptides (Figure S3A-E, Table S3).Totally, We identified a total of 4880 unique Kac sites on 1370 proteins, with various numbers of modification sites on each quantified protein.

At ZT4, 12 up-regulated differentially expressed acetylation sites (DEASs) in 12 proteins and 207 down-regulated DEASs in 157 proteins were identified in the SR group versus CON group, indicating SR-induced extensively inhibition of the Kac modification; conversely, 369 up-regulated DEASs in 228 proteins and 40 down-regulated DEASs in 40 proteins were identified in the SR+PTE versus SR group (*P* value < 0.05, fold change > 1.3 or < 0.77, Figure 5A, 5B, S3F, Table S4), suggesting the probable role of PTE in mitigating SR-induced Kac inhibition. Comparisons of the enriched motifs for Kac DEASs indicate that threonine (T) was overrepresented, whereas glutamic acid (E) and glutamine (Q) reduced at the -1 and +1 position (Figure S3G, S3H, Table S5, S6). The cellular distribution of DEAPs revealed that nearly 50% DEAPs were located in the mitochondria (Figure 5C, Table S7-1), which implied that most DEAPs were associated with metabolic process in the rest phase.

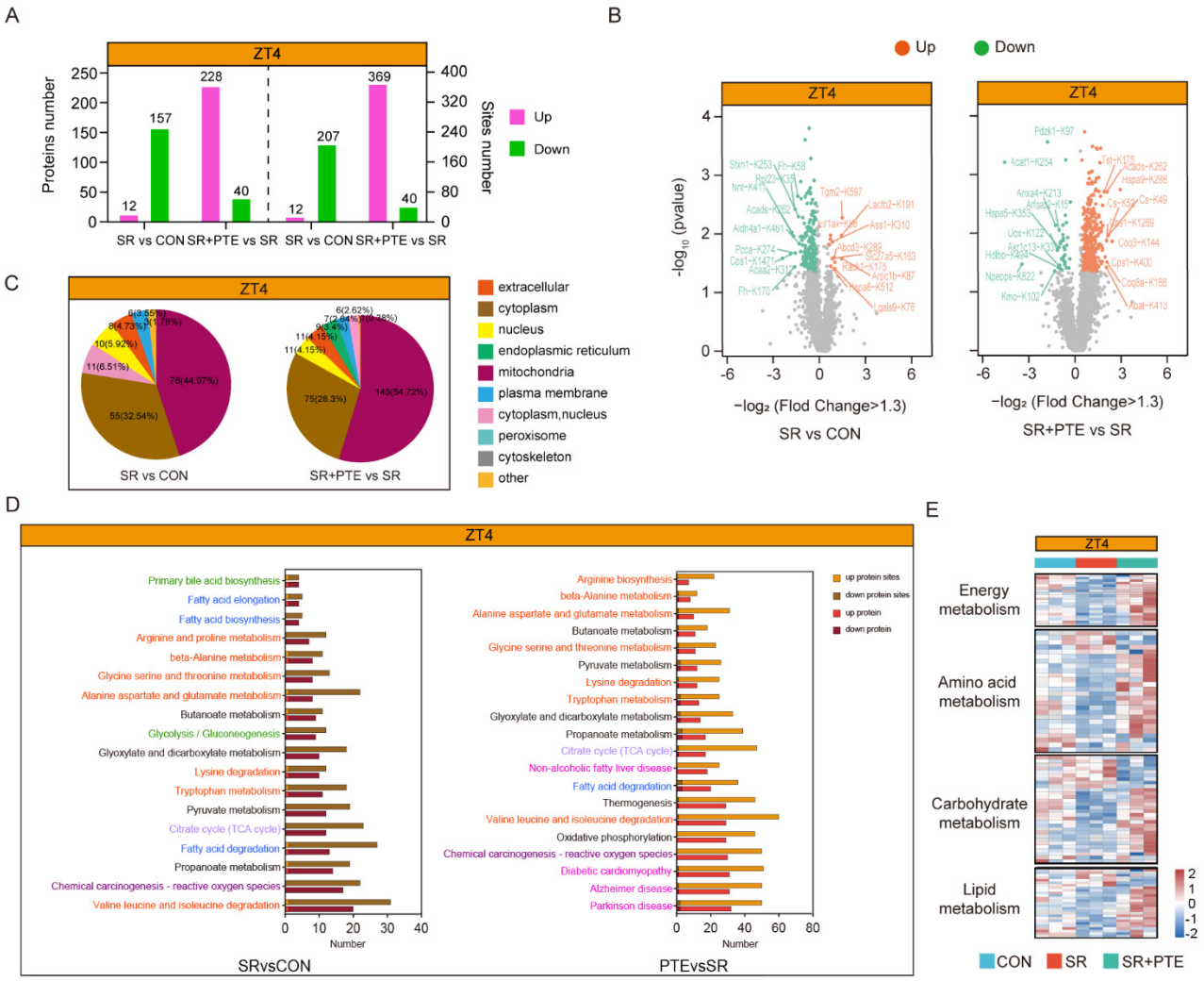

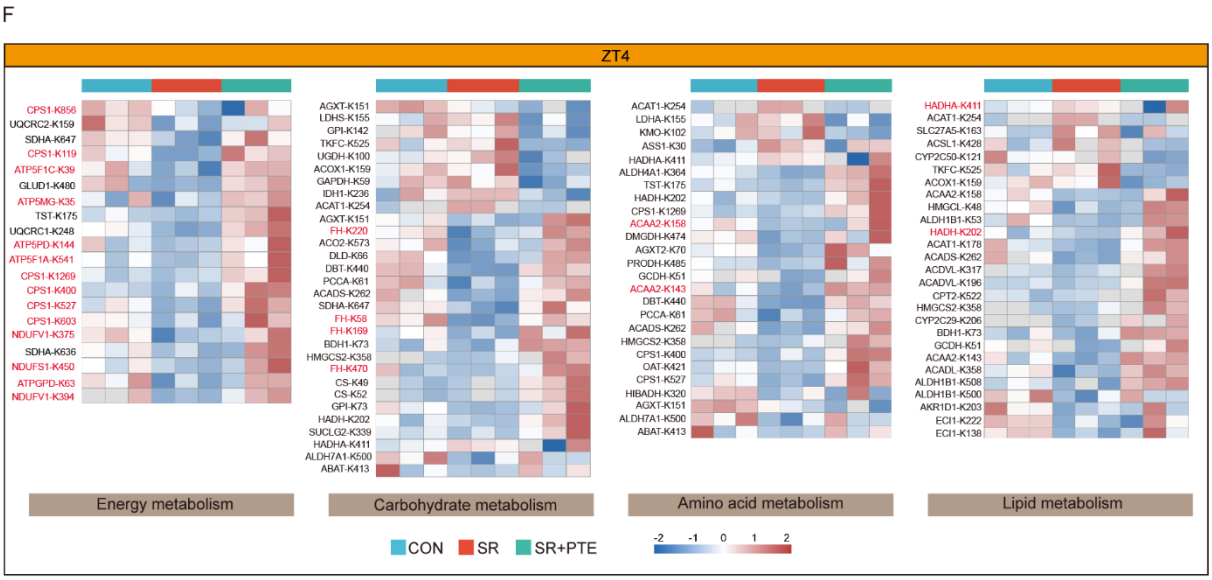

Figure 5. PTE altered the comprehensive landscape of Kac in the liver of SR mice at ZT4.

(A) Statistical analysis of Kac-modification proteins and differentially expressed sites in livers of three groups mice (*P* value < 0.05, fold change > 1.3 or < 0.77). (B) The volcano plots show the top 10 upregulated and downregulated Kac modification sites. (C) Subcellular distribution of Kac-modified proteins. (D) KEGG biological process enrichment analysis indicated the significant enrichment of differentially expressed Kac-modified proteins. (E) Heatmap visualizes the changes in metabolism-related proteins analysed by Kac modification the proteomic databases, including energy, amino acid, carbohydrate and lipid metabolism. (F) The most significant differentially expressed sites and proteins were shown as classification heatmaps related to the pathways indicated in (E).

Kyoto Encyclopedia of Genes and Genomes (KEGG) enrichment analysis further revealed that the DEAPs were involved in multiple biological processes and pathways, mainly in metabolic processes (Figure 5D, Table S8 1-2). In SR mice, when compared with the CON group, the top20 differential Kac modifications were occurred on most metabolic metabolism pathways including lipid metabolism (such as fatty acid biosynthesis, degradation, digestion & absorption), amino acid metabolism (such as valine, leucine, lysine, alanine, aspartate, glutamate, beta-alanine, arginine and proline, isoleucine and tryptophan metabolism), glucose metabolism (such as glycolysis & gluconeogenesis), and TCA cycle. Additionally, the differential Kac modifications in "reactive oxygen species" pathway were observed in SR mice. In PTE group, when compared with SR mice, the above metabolic related pathways and "reactive oxygen species" pathway altered in SR mice were significantly altered. Interestingly, "Thermogenesis pathway" and several chronic diseases related pathways such as "Non-alcoholic fatty liver disease", "Alzheimer disease", "Parkinson disease", and "Diabetic cardiomyopathy" were also significantly altered in PTE group, which might suggest the important role of PTE in chronic disease prevention.

Furthermore, specific cluster analysis showed the alterations of DEAPs at ZT4 involved in the "Energy metabolism", "Amino Acid metabolism", "Lipid metabolism" and "Carbohydrate metabolism" were remarkably different among the three experimental groups (Figure 5E), and the most changed DEAPs in those clusters were displayed in Figure 5F . For example, we can clearly demonstrated that PTE could mitigate SR-induced inhibition of Kac modifications of carbamoyl-phosphate synthase (CPS1), NADH: Ubiquinone Oxidoreductase Core Subunit V1 (NDUFV1) and several subunits of ATP Synthase (ATP5) in "Energy

metabolism" cluster, Fumarate Hydratase (FH) in "Carbohydrate metabolism" cluster, acetyl-CoA acyltransferase 2 (ACAA2) in "Amino acid metabolism" and Hydroxyacyl-CoA Dehydrogenase (HADH) in "Lipid metabolism". Notably, most of the top 20 DEAPs were almost located in mitochondrion, suggesting the important role of PTE on Kac modification in mitochondrial proteins.

In summary, PTE could improve SR-induced metabolic disorders at the rest phase, with significantly mitigating the abnormal Kac modification inhibition in SR mice liver.

3.5 PTE altered the comprehensive landscape of Kac in the liver of SR mice at ZT16

To further investigate the diurnal liver function regulated by PTE, the Kac proteomic analysis was also performed at the active phase ZT16. Among the Kac sites, the 46 DEASs in 44 DEAPs were up-regulated and 110 DEASs in 101 DEAPs were down-regulated in the SR group versus the CON group, implying that SR extensively disturbed Kac modifications with nearly 2/3 down-regulated and 1/3 up-regulated DEAPs. Conversely, the 188 DEASs in 152 DEAPs up-regulated and 76 DEASs in 67 DEAPs down-regulated were identified in the SR+PTE versus SR group, indicating the probable role of PTE in mitigating SR-induced Kac modification disturbance (P value < 0.05, fold change > 1.3 or < 0.77, Figure 6A, 6B, S3F, Table S4). The cellular distribution of the DEAPs showed that more than 40% DEAPs located in the cytoplasm and about 30% DEAPs located in the mitochondria (Figure 6C and Table S7-2.), demonstrating that Kac modification participated in more extensive biological processes in the active phase.

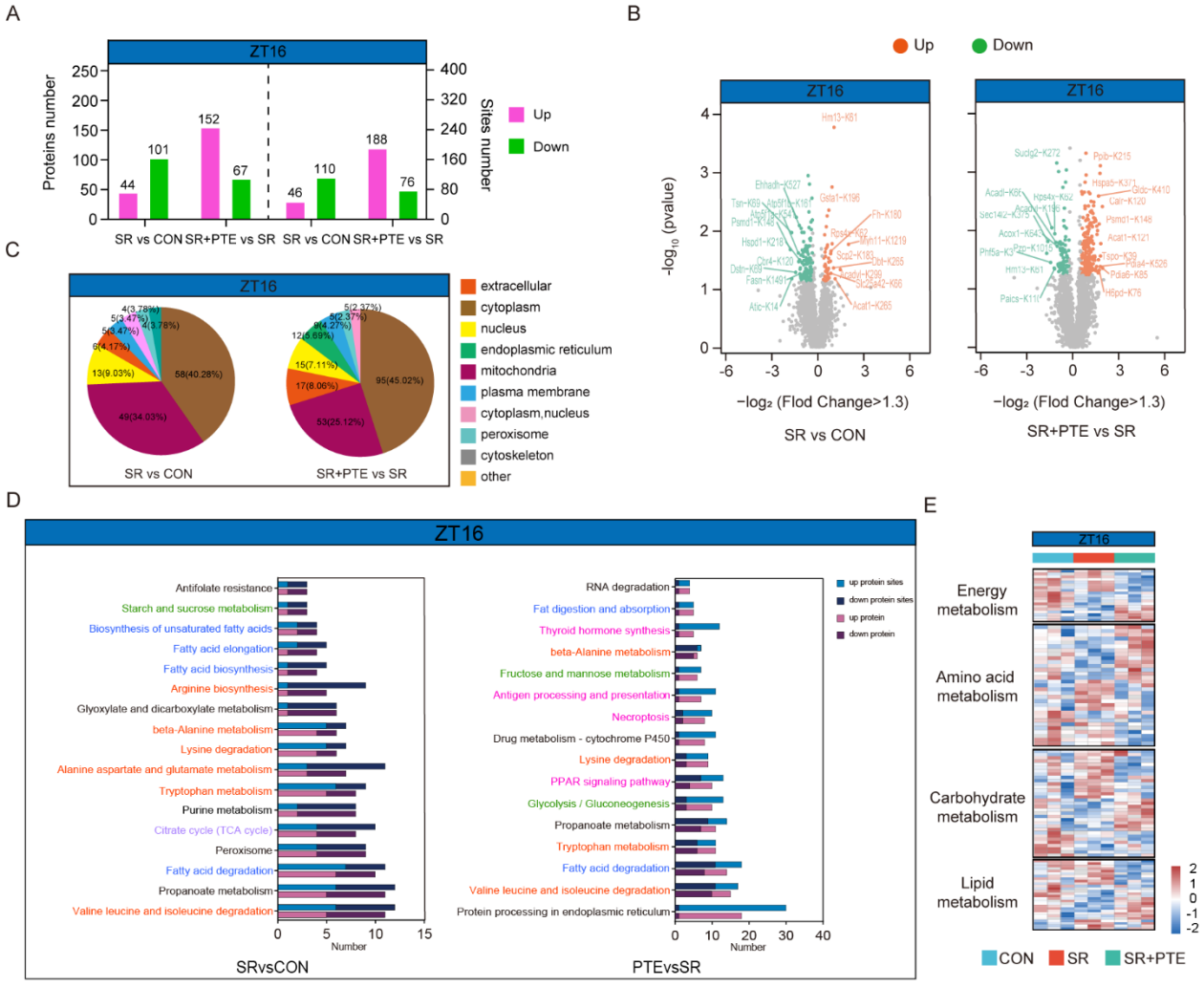

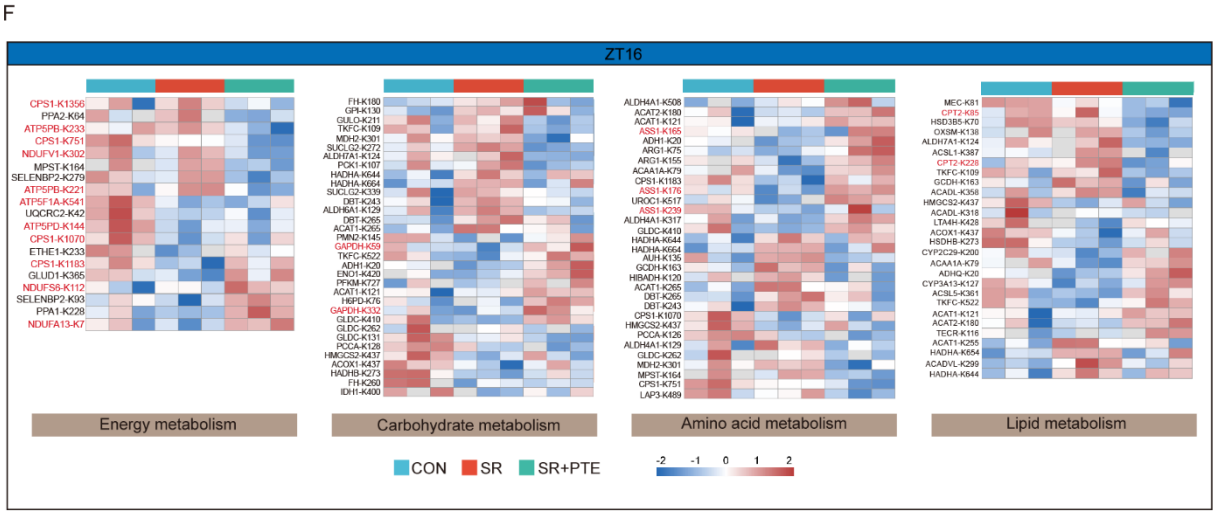

Figure 6. PTE altered the comprehensive landscape of Kac in the liver of SR mice at ZT16.

(A) Differentially expressed Kac-modification sites and proteins in the livers at ZT16 (P value < 0.05, fold change > 1.3 or < 0.77). (B) The top 10 significantly changed differentially expressed Kac-modification sites was shown in the volcano plots. (C) Subcellular distribution of Kac-modified proteins. (D) Analysis of biological process of Kac proteins by KEGG enrichment. (E) Four major distinct proteomic subgroups associated with metabolism were displayed in the heatmap. (F) The most significant differentially expressed sites and proteins were shown as classification heatmaps related to the pathways indicated in (E).

KEGG enrichment analysis results were shown in Figure 6D & Table S8 3-4. In SR mice, when compared with the CON group, the top20 differential Kac modifications were still occurred on metabolic pathways like ZT4, including lipid metabolism, amino acid metabolism, glucose metabolism, and TCA cycle. In PTE group, when compared with SR mice, the above metabolic related pathways altered in SR mice were significant different. Interestingly, “PPAR signaling pathway”, “Thyroid hormone synthesis”, “Antigen processing and presentation” and “Necroptosis” were significantly altered in PTE group, which might indicate the important role of PTE in maintaining metabolic and immunological homeostasis in the active phase.

Further specific cluster analysis showed the alterations of DEAPs at ZT16 involved in the “Energy metabolism”, “Amino Acid metabolism”, “Lipid metabolism” and “Carbohydrate metabolism” were different among the three groups (Figure 6E), and the most changed DEAPs in those clusters were displayed in Figure 6F . For example, we can find that PTE could decrease SR-induced elevation of Kac modifications in CPS1, ATP5 and NDUFV1 in “Energy metabolism” cluster and in carnitine palmitoyltransferase 2 (CPT2) in “Lipid metabolism” cluster at ZT16, which were inhibited in SR mice at ZT4. Meanwhile, we can also find that PTE could reverse SR-induced decrease of Kac modifications of glyceraldehyde phosphate dehydrogenase (GAPDH) in “Carbohydrate metabolism” cluster and argininosuccinate synthase 1 (ASS1) in “Amino acid metabolism” cluster at ZT16, which were elevated in SR mice at ZT4.

In summary, PTE could also improve SR-induced metabolic disorders at the active phase, with significantly mitigating the disturbance of Kac modification in SR mice liver.

3.6 PTE regulated diurnal Kac modification of featured proteins in the liver of SR mice

To further demonstrate the improvement effect of PTE on SR-induced metabolic disorders, 13 simultaneously changed DEAPs in four Kac proteomic data (ZT4 SR vs CON, ZT4 SR+PTE vs SR, ZT16 SR

vs CON, ZT16 SR+PTE vs SR) by Venn analysis (Figure 7A) were presented to analyze their rhythmic Kac modification alterations. These 13 featured DEAPs were related with amino acid metabolism (CPS1, ASS1, ALDH4A1, GCDH, DHTKD1, DBT), lipid metabolism (FASN, ACAT1, HADHA), Citric acid cycle (SUCLG2, MDH2), folate metabolism (ALDH1L1) and stress response (HSPD1). Moreover, a total of 85 DEASs in these 13 featured DEAPs were identified, and 20 acetylation sites simultaneously modified in at least two experimental groups in 11 featured proteins were further analyzed to reveal their circadian alterations (Table S9).

A

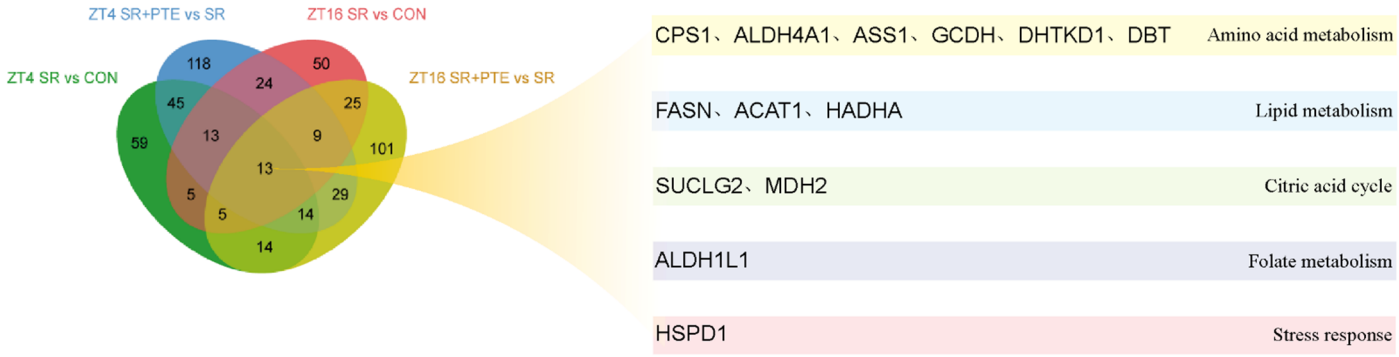

B

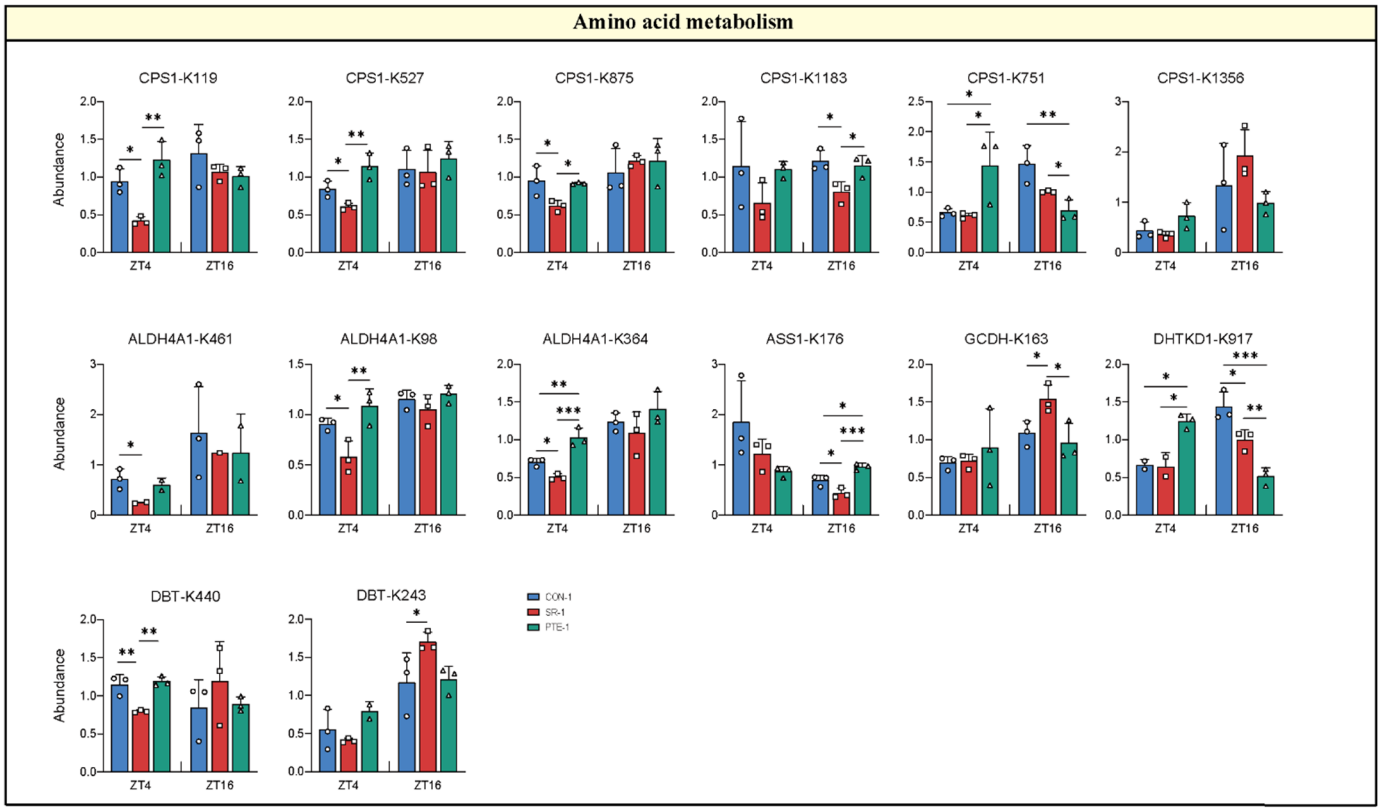

C

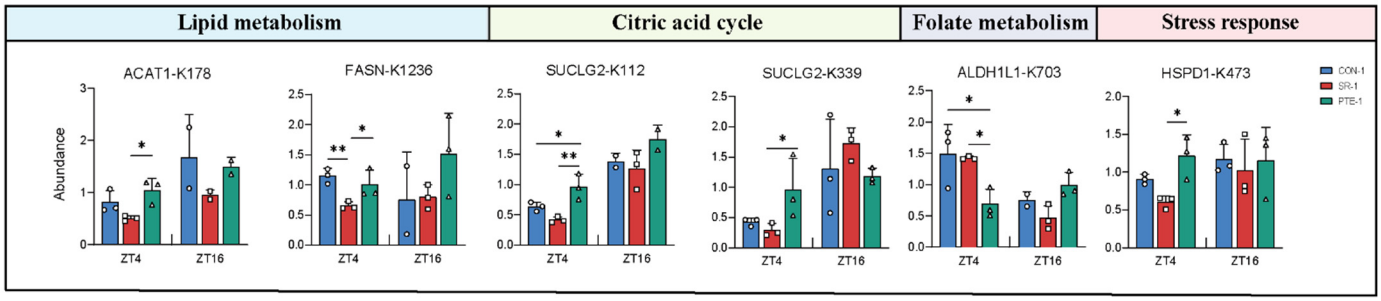

Figure 7. PTE regulated diurnal Kac modification of featured proteins in the liver of SR mice.

(A) Venn diagram showing the overlapped 13 differential Kac-modification proteins in four Kac proteomic data; (B) Specific examples in "amino acid metabolism" cluster to display diurnal alterations in the same Kac sites of CPS-1, ALDH4A1, ASS1, GCDH, HTDKD1 and DBT under SR condition at ZT4 and ZT16. (C) Specific examples in "lipid metabolism", "Citritic acid cycle", "Folate metabolism" and "Stress response" clusters to display diurnal alterations in the same Kac sites of ACAT1, FASN,SUCLG2, ALDH1L1 and HSPD1 under SR condition at ZT4 and ZT16. Data are expressed as the mean ± SD. Statistics were performed with one-way ANOVA, $*P < 0.05$, $**P < 0.01$.

Specific examples in "amino acid metabolism" cluster were shown in Figure 7B. Firstly, CPS1, a mitochondrial enzyme that catalyzes the first step in the urea cycle by producing carbamoyl phosphate. Multiple sites of acetylation were detected for CPS1, basically, low acetylation levels of CPS1 during the rest phase ZT4 that elevated at the active phase ZT16 in the livers of control mice. Notably, PTE were observed to significantly increase SR-induced inhibition of the acetylation in CPS-K119, CPS-K527and CPS-K875 at ZT4, and CPS-K1183 at ZT 16. Secondly, the ALDH4A1, a mitochondrial matrix NAD-dependent dehydrogenase, catalyzes the second step of the proline degradation pathway. Multiple sites of acetylation were also detected for ALDH4A1, and lower acetylation levels of ALDH4A1 at the rest phase while higher at the active phase. Likewise, PTE significantly increased SR-induced inhibition of the acetylation in ALDH4A1-K461, ALDH4A1-K364 and ALDH4A1-K98 at ZT4. Thirdly, previous studies[24] have proved that clock mediated the acetylation of ASS1-K165 and ASS1-K176 directly, and the acetylation of ASS1 exhibited pronounced rhythmicity with peaks at ZT12 and troughs at ZT0 in mouse liver. In our study, SR inhibited the acetylation of ASS1-K176 while PTE administration significantly increased its acetylation. Fourth, the GCDH, existed in the mitochondrial matrix, catalyzes the oxidative decarboxylation of glutaryl-CoA to crotonyl-CoA and CO_2 in the degradative pathway of L-lysine, L-hydroxylysine, and L-tryptophan metabolism. PTE were observed to significantly decrease SR-induced elevation of the acetylation in GCDH-K163 at ZT16. Additionally, the acetylation of DHTKD1 and DBT, two enzymes respectively involved in the degradation pathways of lysine and branched-chain amino acids, had some alterations in PTE group but without significant pattern. According to the above specific examples, PTE might play an important role in mitigating the disturbance of rhythmic acetylation of amino acid metabolism, especially on amino acid degradation.

Specific examples in "Lipid metabolism" cluster were shown Figure 7C. Firstly, ACAT1, one of the enzymes that catalyzes the last step of the mitochondrial beta-oxidation pathway, an aerobic process breaking down fatty acids into acetyl-CoA. Notably, PTE were observed to significantly increase SR-induced inhibition

of the acetylation in ACAT-K178 at ZT4. Secondly, FASN, its main function is to catalyze the synthesis of palmitate from acetyl-CoA and malonyl-CoA into long-chain saturated fatty acids,PTE were observed to significantly increase SR-induced inhibition of the acetylation in FASN-K1236 at ZT4. Other specific examples in “Citric acid cycle”, “Folate metabolism” and “Stress response” clusters were shown Figure 7C. SUCLG2 catalyzes the reversible reaction involving the formation of succinyl-CoA and succinate. In this study, PTE were observed to significantly increase SR-induced inhibition of the acetylation in SUCLG2-K112 at ZT4. Meanwhile, PTE was observed to change the acetylation levels of ALDH1L1 (the key enzyme catalyzes the conversion of 10-formyltetrahydrofolate to tetrahydrofolate) and HSPD1 (also called HSP60) at ZT4 under SR condition.

Taken together, PTE could improve the disrupted rhythmic Kac modification of featured proteins in the liver of SR mice, which is critical for mitigating SR-induced metabolic disorders.

3.7 PTE promoted the diurnal activity of SIRT1 and SIRT3 in the liver of SR mice

The dynamic balance of Kac modification is maintained by protein acetylation and deacetylation, regulated by enzymatic activities of HATs and HDACs respectively. To determine the effect of PTE on lysine deacylases, we focused on SIRT1 and SIRT3, widely known as the NAD^+-dependent sirtuins with strong deacetylase activity in cell nucleus and mitochondria. We measured NAD^+/NADH at seven zeitgeber time points and found that PTE effectively restored the circadian oscillation of NAD^+/NADH content in SR mouse livers (Figure 8A). RT-qPCR and immunoblotting analysis illustrated a rhythmic expression of NAD^+ synthetase NAMPT under PTE intervention in the liver of SR-treated mice (Figure 8B). Moreover, PTE significantly retained SIRT1 activity in the liver of SR group at ZT4, but neither at ZT16 nor in vitro without additional NAD^+ (Figure 8C-8E, S5). PTE intervention potently raised SIRT1 mRNA and protein expression in response to SR, and similar results were observed in SIRT3 (Figure 8F, 8G, Table S10). These results indicated that maintaining the rhythmic oscillation of SIRT1/3 was the potential mechanism of PTE in improving the liver Kac modification disruption under SR condition.

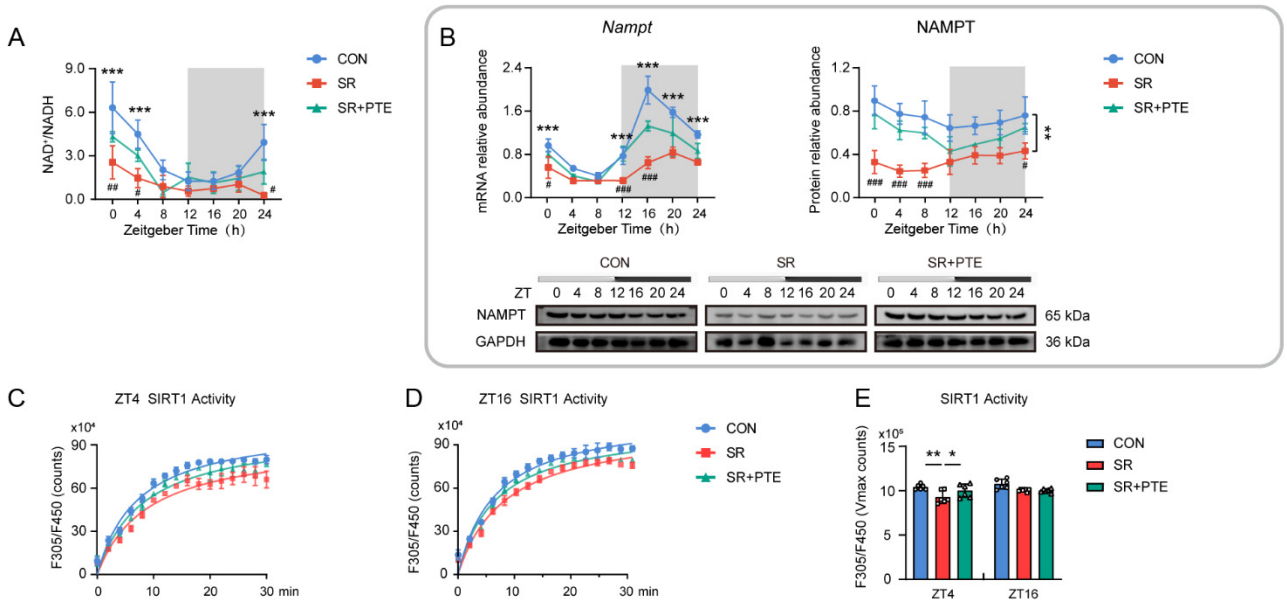

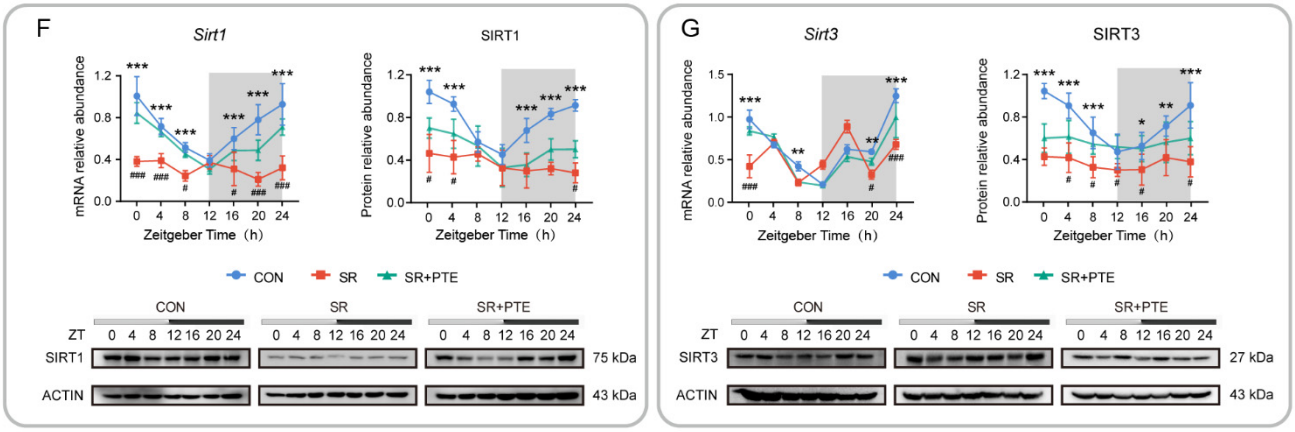

Figure 8. PTE promoted the functional activity of SIRT1 and SIRT3 in the liver of SR mice.

(A) Dynamic changes of NAD^+/NADH in the livers during SR induced with PTE treatment (n=4). (B) Transcription level and protein expression of NAD^+ synthetase NAMPT was measured by RT-qPCR and western blotting (n=4). (C-E) Liver samples collecting from three groups at ZT4 and ZT16 were used to determine the activity of SIRT1 (n=4). (F,G) The mRNA levels and protein expressions of SIRT1 and SIRT3 were modulated as diurnal rhythm oscillating (n=4). Data are expressed as the mean ± SD. Statistics were performed with one-way ANOVA and two-way ANOVA, $^*P < 0.05$, $^{**}P < 0.01$, $^{***}P < 0.001$, and $^*P < 0.05$, $^{**}P < 0.01$, $^{***}P < 0.001$, CON group versus SR group, $^{\#}P < 0.05$, $^{\#\#}P < 0.01$, $^{\#\#\#}P < 0.001$, SR+PTE group versus SR group.

4. Discussion

Sleep deficiency disrupts circadian rhythms to trigger numerous pathological processes including metabolic disorders. In this study, we confirmed that PTE improved systemic energy homeostasis, liver metabolic and mitochondria function of mice subjected to 5-days' SR in a diurnal range. Notably, a comprehensive resource detailing the acetylation modifications in mouse liver exposed to sleep deficiency was firstly presented, and simultaneously provided substantial evidence to illustrate the protective mechanisms of PTE on SR-induced metabolic disorders. Moreover, PTE was observed to normalize the diurnal expression and activity of deacetylases SIRT1/3 by maintaining NAD^+ oscillation, which might directly contribute to acetylation modulation. Therefore, this study also deepened our understanding of PTE's functional mechanisms and broadened its biological significance.

PTE is a naturally-derived phytoalexin produced by plants in response to exposure to ultraviolet light or microbial infection. It is predominantly found in blueberries, peanuts, several types of grapes, and some tree woods. A study conducted to determine the presence of PTE in *Vaccinium* berries showed that PTE was found at levels of 99−520 ng/g dry sample [25]. In addition, PTE is abundant in the *Chinese dragon's blood*, a rare and valuable traditional Chinese medicine with a long history of medical use, which reaches up to 2-4 mg/g [26]. These quantitative analyses add to the purported health benefits derived from the consumption of these small fruits and the utilization of traditional Chinese medicine. As the increasing attention have been focused on PTE as a health-promoting nutraceutical, its absorption, metabolism, tissue distribution, and excretion have been well studied [27-28]. Besides be absorbed directly in intestine, PTE and its major metabolites i.e. PTE sulfate, and hydroxylated PTE were identified and quantified in the mucosa and content of the digestive tissues, blood, urine and vital organs including the liver. Thus, the universal distribution of PTE provides the basis for its versatile beneficial roles.

It has been widely recognized the health-promoting properties of PTE including anti-obesity, anti-inflammation, protecting against cancer[7,10]. In our previous study[12], we have primarily identified that PTE could mitigate SR-induced metabolic disorders. And in this study, we further revealed that PTE could reduce the elevation fat mass, the excessive fat accumulation within the liver on condition of the remarkable body weight loss under SR, indicating its role in modulating metabolism particularly in the lipid metabolism. Recently, several studies have reported that PTE could maintain energy metabolic homeostasis *via* increasing oxygen consumption and energy expenditure, and promoting browning of white adipose tissue or activation of brown adipose tissue in both genetic-obesity and diet-induced obesity mouse models[29-30]. With the metabolic monitoring data, we found that, unlike the obesity-related high O_2 consumption, PTE intervention significantly reduced CO_2 exhalation, RER and heat production of SR mice in the rest phase but not the active phase, suggesting its effectiveness on enhancing lipid consumption and maintaining the balance of metabolic substrate utilization. Consistent with the systemic metabolic ameliorations in the rest phase, PTE administration could significantly increase the transcription and expression of lipid transcription factors and lipid metabolic enzymes in liver including PPARα/γ (lipolysis), ACC, HMGCR2 (lipogenesis) and PFK, GCK (glycolysis) at ZT4 or even at ZT16, with the corresponding inhibition of glycolysis process at ZT4. Additionally, according to the effects of PTE on reduction in the loss of body weight and lean mass, and on recovery of the Kac modification oscillation in key enzyme in urea cycle CPS-1, we consider that PTE might also alleviate abnormal protein degradation under SR condition. Moreover, beyond modulation of the metabolic biological processes, PTE could also maintain mitochondrial dynamics at ZT4 and ZT16, and thus played the hepatoprotective role with relieving the mitochondrial injury and the liver dysfunction under SR. Meanwhile, as mitochondrial injury is linked to ectopic fat accumulation and mitochondrial dynamics imbalance. Similar to the results that PTE upgraded the gene expression of PPARα agonist in obese mouse models[31-32].A previous clinical trial has illustrated that 6-months intervention of nicotinamide riboside and pterostilbene could attenuate hepatic inflammation in the NAFLD patients[33], our study revealed that short term PTE supplementation could also be sufficient to improve metabolic disorders.

PTMs play essential roles in numerous physiological and pathological processes. As many metabolites are substrates for enzymes involved in PTM pathways, fluctuations in metabolite levels might directly affect histone and non-histone protein modifications. Previous studies have proved that disruption of the clock may result in a number of changes in the circadian profile of metabolites[31]. How the metabolites involved in the various lysine acylations under SR condition was of great interest. In this study, we primarily found that some alterations of the 11 types of lysine PTMs in the livers from SR mice at ZT4 and ZT16. Beyond the acetylation, the crotonyllysine and the β-hydroxybutyrlysine were also seemed to oscillate diurnally and affected by PTE. As we have observed the Kac modification changes in the crotonyl generating enzymes GCDH or ACADS[32], and previous research reported that the serum level of ketone body β-hydroxybutyrate decreased in volunteers subjected to 32.5-h sleep deprivation[34], it would be interesting to further examine SR-induced crotonyllysine and hydroxybutyrlysine alterations.

Lysine acetylation modification is a well-studied PTM [35-36]. Acetyl-coenzyme A can be used for Kac by acetyltransferase through the mitochondrial oxidation of carbon sources such as glucose, amino acids, and fatty acids, and Kac is under circadian clock control and exhibits circadian rhythm oscillation [16,37-38]. A number of unique oscillated acetylation sites have been identified in WT and clock-/- mouse livers, mainly enriched in the mitochondrial proteins, amino acid metabolism and lipid metabolism[16]. In this study, a total of 1370 proteins were found to be acetylated, with 4880 unique sites of acetylation, which were nearly 10 fold proteins to the previous finding in ten years ago. Notably, we have mapped diurnal Kac proteome profiles at both the rest phase and the active phase, and this dataset would expand our understanding in diurnal acetylation on biological process. In the rest period, nearly 50% of acetylation occurred in mitochondria proteins, indicating that energy and nutrients metabolism dominated. While in the active period, about 40% and 30% acetylation occurred in the cytoplasm and mitochondrial respectively, suggesting that acetylation was involved in more physiological processes when compared with the rest period. Furthermore, under our SR experimental paradigm, we revealed that the disruption of acetylation was more severe at ZT4, which was associated with that SR directly broke the original sleep-wake cycle in mice. According to the KEGG analysis, inhibited amino acid metabolism, lipid metabolism, carbohydrate metabolism and energy metabolism pathways accompanied with disturbed reactive oxygen species pathway were remarkably altered in SR mice, obviously displaying the acetylation profiles of the mice liver respond to sleep deficiency. Further, the KEGG analysis results provided substantial evidences to demonstrating that PTE could not only modulate SR-induced metabolic pathways but also involve in prevention the chronic metabolic related diseases including non-alcoholic fatty liver disease[39], Alzheimer disease[40], Parkinson disease[41] and Diabetic cardiomyopathy[42], which were consistent with many recent researches.

In this study, detailed analysis of the changes in each acetylation site and protein further confirmed that PTE could counteract SR-induced acetylation disturbance. For example, PTE increased SR-induced inhibition of the acetylation in Acat-K178 and Fasn-K1236 at ZT4. Conversely, SR-induced elevation of the acetylation in Gcdh-K163 at ZT16 could be reduced by PTE. Moreover, besides the single site modified in one protein, multiple Kac sites were also identified to have positive effects. For example, PTE could increase SR-induced inhibition of the acetylation in CPS-K119, CPS-K527and CPS-K875 at ZT4, and CPS-K1183 at ZT16. Unfortunately, although we firstly displayed that numerous identified functional proteins with single or multiple acetylation sites were heavily influenced by SR and PTE treatment, it remains largely unknown that the significance of those Kac modifications to the activities of those proteins and the whole metabolism due to the scarce annotations to those acetylation sites. Therefore, more work should put forward to further elaborate the relationship between the site-specific Kac modification and protein function status.

As the global alterations in Kac profile, it's impossible to simply attribute the beneficial effects of PTE to its direct action. The regulation of acetylation is regulated by the writers and erasers. SIRT1 and SIRT3 are the well-known erasers of PTMs, and they distribute in the nucleus and mitochondrial respectively[43-44]. Some evidences prove that PTE directly activated SIRTs in many disease models. For example, PTE increased

browning effects and mitochondrial biogenesis though SIRT1/PGC-1α/SIRT3 pathway to inhibit diet-induced obesity[9,45]. An oxidative stress-induced amyotrophic lateral sclerosis study reports the PTE remarkably raised the expression and activity of SIRT1 and SIRT3[46]. Our previous study found that PTE upregulated PGC1α acetylation level though SIRT1 activity in SR mouse skeletal muscle[11]. In this study, we also found that PTE improved the rhythmic expression of SIRT1 and SIRT3 though maintaining the content of NAD^+/NADH in SR mouse liver. Actually, the diurnal oscillation of NAD^+/NADH content benefited by circadian rhythm of NAMPT, and PTE was determined to restore the rhythmic expression of NAMPT under SR. Overall, we further confirmed the positive influence on the landscape of Kac modification of PTE was correlated with circadian modulation though activating SIRT1 and SIRT3 under SR condition.

In conclusion, this study confirmed the protective effect of PTE on metabolic disorders under SR condition, especially significant improvements in abnormal lipid accumulation and mitochondrial dysfunction in the liver. Importantly, we constituted a dataset deciphering the diurnal acetylation modifications in mouse liver when exposed to sleep restriction, and firstly revealed the metabolic improving mechanism in the PTMs modulation perspective. Moreover, PTE was observed to normalize the diurnal expression and activity of deacetylases SIRT1/3 by maintaining NAD^+ oscillation, which might directly contribute to acetylation modulation. Therefore, this study dramatically expanded our understanding of PTE's functional mechanisms, and it would laid the foundation for exploration more drugs to ameliorate SR-induced metabolic disorders.

Acknowledgements

This research was supported by the research grants from National Natural Science Foundation of China (NSFC82073548).

Data Availability Statement

Raw data of the acetylome analysis for the diurnal acetylation modifications in mouse liver will be available by the corresponding author upon reasonable request.

Conflicts of interest

The authors declared that no conflict of interests.

References

[1] C. Antza, G. Kostopoulos, S. Mostafa, et al., The links between sleep duration, obesity and type 2 diabetes mellitus, J. Endocrinol. 252 (2021) 125-141. https://doi.org/10.1530/JOE-21-0155.

[2] N. Covassin, P. Singh, S.K. McCrady-Spitzer, et al., Effects of experimental Sleep Restriction on energy intake, energy expenditure, and visceral obesity, J. Am. Coll. Cardiol. 79 (2022) 1254-1265. https://doi.org/10.1016/j.jacc.2022.01.038.

[3] J.-P. Chaput, A.W. McHill, R.C. Cox, et al., The role of insufficient sleep and circadian misalignment in obesity, Nat. Rev. Endocrinol. 19 (2023) 82-97. https://doi.org/10.1038/s41574-022-00747-7.

[4] J. Peng, C. Lu, Y. Luo, et al., Hypoglycemic effects and associated mechanisms of resveratrol and related stilbenes in diet, Food Funct. 15 (2024) 2381-2405. https://doi.org/10.1039/d3fo04761j.

[5] X. Liao, J. Zou, M. Wu, et al., Hypoglycemic effect of nobiletin via gut Microbiota-metabolism axis on hyperglycemic mice, Mol. Nutr. Food Res. 67 (2023) e2200289. https://doi.org/10.1002/mnfr.202200289.

[6] Y.-C. Koh, P.-S. Lee, Y.-L. Kuo, et al., Dietary pterostilbene and resveratrol modulate the gut Microbiota influenced by circadian rhythm dysregulation, Mol. Nutr. Food Res. 65 (2021) e2100434. https://doi.org/10.1002/mnfr.202100434.

[7] H. Kim, K.-H. Seo, W. Yokoyama, Chemistry of pterostilbene and its metabolic effects, J. Agric. Food Chem. 68 (2020) 12836-12841. https://doi.org/10.1021/acs.jafc.0c00070.

[8] Z.T. Zhang, S.M. Deng, C. Chen, et al., Pterostilbene could alleviate diabetic cognitive impairment by suppressing TLR4/NF-κkB pathway through microbiota-gut-brain axis, Phytother Res 37 (2023) 3522-3542. https://doi.org/10.1002/ptr.7827.

[9] Y.C. Koh, S.J. Lin, K.Y. Hsu, et al., Pterostilbene Enhances Thermogenesis and Mitochondrial Biogenesis by Activating the SIRT1/PGC-1alpha/SIRT3 Pathway to Prevent Western Diet-Induced Obesity, Mol Nutr Food Res 67 (2023) e2300370. https://doi.org/10.1002/mnfr.202300370.

[10] B. Özyalçın, N. Sanlier, Antiobesity pathways of pterostilbene and resveratrol: a comprehensive insight, Crit. Rev. Food Sci. Nutr. 64 (2024) 11428-11436. https://doi.org/10.1080/10408398.2023.2238319.

[11] Y. Liu, H. Lang, M. Zhou, et al., The preventive effects of pterostilbene on the exercise intolerance and circadian misalignment of mice subjected to sleep restriction, Mol. Nutr. Food Res. 64 (2020) e1900991. https://doi.org/10.1002/mnfr.201900991.

[12] J. Zhang, M. Chang, X. Wang, et al., Pterostilbene targets the molecular oscillator RORgamma to restore circadian rhythm oscillation and protect against sleep restriction induced metabolic disorders, Phytomedicine 125 (2024) 155327. https://doi.org/10.1016/j.phymed.2023.155327.

[13] A. Dutta, S.M. Abmayr, J.L. Workman, Diverse activities of histone acylations connect metabolism to chromatin function, Mol. Cell 63 (2016) 547-552. https://doi.org/10.1016/j.molcel.2016.06.038.

[14] M.S. Robles, J. Cox, M. Mann, In-vivo quantitative proteomics reveals a key contribution of post-transcriptional mechanisms to the circadian regulation of liver metabolism, PLoS Genet. 10 (2014) e1004047. https://doi.org/10.1371/journal.pgen.1004047.

[15] J. Hirayama, S. Sahar, B. Grimaldi, et al., CLOCK-mediated acetylation of BMAL1 controls circadian function, Nature 450 (2007) 1086-1090. https://doi.org/10.1038/nature06394.

[16] S. Masri, V.R. Patel, K.L. Eckel-Mahan, et al., Circadian acetylome reveals regulation of mitochondrial metabolic pathways, Proc. Natl. Acad. Sci. U. S. A. 110 (2013) 3339-3344. https://doi.org/10.1073/pnas.1217632110.

[17] M. Shvedunova, A. Akhtar, Modulation of cellular processes by histone and non-histone protein acetylation, Nat. Rev. Mol. Cell Biol. 23 (2022) 329-349. https://doi.org/10.1038/s41580-021-00441-y.

[18] H. Jiang, X. Wang, J. Ma, G. Xu, The fine-tuned crosstalk between lysine acetylation and the circadian rhythm, Biochim. Biophys. Acta Gene Regul. Mech. 1866 (2023) 194958. https://doi.org/10.1016/j.bbagrm.2023.194958.

[19] Q.-J. Wu, T.-N. Zhang, H.-H. Chen, et al., The sirtuin family in health and disease, Signal Transduct. Target. Ther. 7 (2022) 402. https://doi.org/10.1038/s41392-022-01257-8.

[20] C. Lu, H. Zhao, Y. Liu, et al., Novel role of the SIRT1 in endocrine and metabolic diseases, Int. J. Biol. Sci. 19 (2023) 484-501. https://doi.org/10.7150/ijbs.78654.

[21] D. Wang, L. Cao, X. Zhou, et al., Mitigation of honokiol on fluoride-induced mitochondrial oxidative stress, mitochondrial dysfunction, and cognitive deficits through activating AMPK/PGC-1α/Sirt3, J. Hazard. Mater. 437 (2022) 129381. https://doi.org/10.1016/j.jhazmat.2022.129381.

[22] Y. Shao, X. Wang, Y. Zhou, et al., Pterostilbene attenuates RIPK3-dependent hepatocyte necroptosis in alcoholic liver disease via SIRT2-mediated NFATc4 deacetylation, Toxicology 461 (2021) 152923. https://doi.org/10.1016/j.tox.2021.152923.

[23] L. Chen, Q. Zhang, Y. Meng, et al., Saturated fatty acids increase LPI to reduce FUNDC1 dimerization and stability and mitochondrial function, EMBO Rep. 24 (2023) e54731. https://doi.org/10.15252/embr.202254731.

[24] R. Lin, Y. Mo, H. Zha, et al., CLOCK acetylates ASS1 to drive circadian rhythm of ureagenesis, Mol. Cell 68 (2017) 198-209.e196. https://doi.org/10.1016/j.molcel.2017.09.008.

[25]A.M. Rimando, W. Kalt, J.B. Magee, et al., Resveratrol, pterostilbene, and piceatannol in berries, J Agr Food Chem 52 (2004) 4713-4719. https://doi.org/10.1021/jf040095e.

[26] X.T. Sun, Q. Huang, M.S. Wu, et al., Metabolomics and quantitative analysis to determine differences in the geographical origins and species of Chinese dragon's blood, Front Plant Sci 15 (2024). https://doi.org/ARTN 142773110.3389/fpls.2024.1427731.

[27] L.D. Zhang, G.L. Tian, L. Huang, et al., Pterostilbene attenuates intestinal epithelial barrier loss induced by high loading intensity of exercise, Front Nutr 9 (2022). https://doi.org/ARTN 96518010.3389/fnut.2022.965180.

[28] Y. Sun, Q. Wang, X. Wu, et al., Gastrointestinal biotransformation and tissue distribution of pterostilbene after long-term dietary administration in mice, Food Chem 372 (2022). https://doi.org/ARTN 13121310.1016/j.foodchem.2021.131213.

[29] Y.-C. Koh, S.-J. Lin, K. Nagabhushanam, et al., The anti-obesity and anti-inflammatory capabilities of pterostilbene and its colonic metabolite pinostilbene protect against tight junction disruption from western diet feeding, Mol. Nutr. Food Res. 66 (2022) e2200146. https://doi.org/10.1002/mnfr.202200146.

[30] L. Aguirre, S. Palacios-Ortega, A. Fernández-Quintela, et al., Pterostilbene reduces liver steatosis and modifies hepatic fatty acid profile in obese rats, Nutrients 11 (2019) 961. https://doi.org/10.3390/nu11050961.

[31] K. Thurley, C. Herbst, F. Wesener, et al., Principles for circadian orchestration of metabolic pathways, Proc. Natl. Acad. Sci. U. S. A. 114 (2017) 1572-1577. https://doi.org/10.1073/pnas.1613103114.

[32] H. Yuan, X. Wu, Q. Wu, et al., Lysine catabolism reprograms tumour immunity through histone crotonylation, Nature 617 (2023) 818-826. https://doi.org/10.1038/s41586-023-06061-0.

[33] R.W. Dellinger, H.E. Holmes, T. Hu-Seliger, et al., Nicotinamide riboside and pterostilbene reduces markers of hepatic inflammation in NAFLD: A double-blind, placebo-controlled clinical trial, Hepatology 78 (2023) 863-877. https://doi.org/10.1002/hep.32778.

[34] S. Liu, X. Ma, Y. Chen, et al., Multiplex influences on vigilance and biochemical variables induced by sleep deprivation, Front. Sports Act. Living 6 (2024) 1412044. https://doi.org/10.3389/fspor.2024.1412044.

[35] D. Zhang, Z. Tang, H. Huang, et al., Metabolic regulation of gene expression by histone lactylation, Nature 574 (2019) 575-580. https://doi.org/10.1038/s41586-019-1678-1.

[36] O. Morales-Tarré, R. Alonso-Bastida, B. Arcos-Encarnación, et al., Protein lysine acetylation and its role in different human pathologies: a proteomic approach, Expert Rev. Proteomics 18 (2021) 949-975. https://doi.org/10.1080/14789450.2021.2007766.

[37] Q. Zhu, W.J. Belden, Molecular regulation of circadian chromatin, J. Mol. Biol. 432 (2020) 3466-3482. https://doi.org/10.1016/j.jmb.2020.01.009.

[38] D. Mauvoisin, F. Atger, L. Dayon, et al., Circadian and feeding rhythms orchestrate the diurnal liver acetylome, Cell Rep. 20 (2017) 1729-1743. https://doi.org/10.1016/j.celrep.2017.07.065.

[39] B. Shen, Y. Wang, J. Cheng, et al., Pterostilbene alleviated NAFLD via AMPK/mTOR signaling pathways and autophagy by promoting Nrf2, Phytomedicine 109 (2023) 154561. https://doi.org/10.1016/j.phymed.2022.154561.

[40] J. Liu, J. Xu, L. Jia, et al., Pterostilbene nanoemulsion promotes Nrf2 signaling pathway to downregulate oxidative stress for treating Alzheimer's disease, Int. J. Pharm. 655 (2024) 124002. https://doi.org/10.1016/j.ijpharm.2024.124002.

[41] Y. Fan, X. He, M. Chen, et al., Pterostilbene alleviates MPTP-induced neurotoxicity by targeting neuroinflammation and oxidative stress, Biochem. Biophys. Res. Commun. 729 (2024) 150358. https://doi.org/10.1016/j.bbrc.2024.150358.

[42] R. Kosuru, V. Kandula, U. Rai, et al., Pterostilbene decreases cardiac oxidative stress and inflammation via activation of AMPK/Nrf2/HO-1 pathway in fructose-fed diabetic rats, Cardiovasc. Drugs Ther. 32 (2018) 147-163. https://doi.org/10.1007/s10557-018-6780-3.

[43] J. Zhang, H. Xiang, J. Liu, et al., Mitochondrial Sirtuin 3: New emerging biological function and therapeutic target, Theranostics 10 (2020) 8315-8342. https://doi.org/10.7150/thno.45922.

[44] M. Wang, H. Lin, Understanding the function of mammalian sirtuins and protein lysine acylation, Annu. Rev. Biochem. 90 (2021) 245-285. https://doi.org/10.1146/annurev-biochem-082520-125411.

[45] M. La Spina, E. Galletta, M. Azzolini, et al., Browning effects of a chronic pterostilbene supplementation in mice fed a high-fat diet, Int. J. Mol. Sci. 20 (2019) 5377. https://doi.org/10.3390/ijms20215377.

[46] E. Obrador, R. Salvador, P. Marchio, et al., Nicotinamide Riboside and Pterostilbene Cooperatively Delay Motor Neuron Failure in ALS SOD1(G93A) Mice, Mol Neurobiol 58 (2021) 1345-1371. https://doi.org/10.1007/s12035-020-02188-7.